Published in final edited form as:
Free Radic Biol Med. 2011 April 15; 50(8): 945–952. doi:10.1016/j.freeradbiomed.2011.01.010.

Primary role of mitochondrial Rieske iron-sulfur protein in hypoxic ROS production in pulmonary artery myocytes

Amit S. Korde, **Vishal R. Yadav**, **Yun-Min Zheng**, and **Yong-Xiao Wang***
Center for Cardiovascular Sciences, Albany Medical College, Albany NY 12208

Abstract

This study was designed to determine whether: (1) hypoxia could directly affect ROS production in isolated mitochondria and mitochondrial complex III from pulmonary artery smooth muscle cells (PASMCs), and (2) Rieske iron-sulfur protein in the complex III might mediate hypoxic ROS production, leading to hypoxic pulmonary vasoconstriction (HPV). Our data, for the first time, demonstrate that hypoxia significantly enhances ROS production, measured by the standard ROS indicator dichlorodihydrofluorescein/diacetate, in isolated mitochondria from PASMCs. Studies using the newly-developed, specific ROS biosensor pHyPer have found that hypoxia increases mitochondrial ROS generation as well in isolated PASMCs. The hypoxic ROS production has also been observed in isolated complex III. Rieske iron-sulfur protein silencing using siRNAs abolishes the hypoxic ROS formation in isolated PASM complex III, mitochondria and cells, while Rieske iron-sulfur protein overexpression produces the opposite effect. Rieske iron-sulfur protein silencing inhibits the hypoxic increase in $[Ca^{2+}]_i$ in PASMCs and hypoxic vasoconstriction in isolated PAs. These findings together provide novel evidence that mitochondria are the direct hypoxic targets in PASMCs, in which Rieske iron-sulfur protein in the complex III may serve as an essential, primary molecule that mediates the hypoxic ROS generation, leading to an increase in $[Ca^{2+}]_i$ in PASMCs and HPV.

Keywords

Mitochondria; Rieske iron-sulfur protein; reactive oxygen species; intracellular calcium; hypoxic pulmonary vasoconstriction

Introduction

Pulmonary arteries (PAs) contract in response to hypoxia, delineated as hypoxic pulmonary vasoconstriction (HPV). This unique response is an important physiological process that optimizes the matching of regional alveolar ventilation to pulmonary perfusion in the lungs, but may also serve as a major pathological factor in the development of pulmonary hypertension. A crucial factor for HPV is an increase in $[Ca^{2+}]_i$ in PA smooth muscle cells (PASMCs) [1].

* **Corresponding author:** Dr. Yong-Xiao Wang Albany Medical College Center for Cardiovascular Sciences (MC-8) 47 New Scotland Avenue Albany, NY 12208 Phone: (518)-262-9506 Fax: (518)-262-8101 wangy@mail.amc.edu.

Pharmacological and genetic studies in PASM cells and tissues indicate that the hypoxic increase in $[Ca^{2+}]_i$ in PASMCs and associated HPV are mediated by ROS signaling, which results from mitochondria and NADPH oxidase (NOX) [1-6]. The NOX-mediated, hypoxic ROS formation is secondary to mitochondrial ROS; this newly-identified ROS-induced ROS generation provides a positive feedback mechanism, contributing to the hypoxic increase in $[Ca^{2+}]_i$ in PASMCs and HPV [7-9]. These findings further demonstrate the importance of mitochondrial ROS in hypoxic cellular responses in PASMCs. Evidence of the essential role of mitochondrial ROS in hypoxic Ca^{2+} and associated contractile responses, together with the fact that mitochondria are the most voracious intracellular oxygen consumers, would seem to indication that mitochondria are the primary hypoxic sensor in PASMCs [1-6]. However, direct experimental evidence to support this view is lacking.

Numerous studies, particularly using isolated mitochondria, have revealed that under physiological conditions, mitochondria may generate ROS predominantly in the electron transport chain (ETC) complex I in most types of cells due to a higher $NADH/NAD^+$ ration in the matrix and/or a higher protonmotive force [10]. As of now, there have been no reports showing ROS formation in isolated mitochondria from PASMCs. Studies in intact cells and tissues using various complex inhibitors suggest that complex III is likely to be the primary site for the hypoxic ROS generation in PASMCs [1-6]. Noticeably, further research is needed to verify the critical, initial role of complex III in PASMCs. Equally importantly, it is necessary to determine which molecule in complex III may serve as a critical factor in the initiation of hypoxic ROS generation in PASMCs.

In this study, thus, we sought to determine whether hypoxia could directly affect ROS generation in isolated mitochondria and complex III from PASMCs. As Rieske iron-sulfur protein is a major functional component of the complex III [11], we also wanted to test whether this molecule could play an important role in the hypoxic ROS generation in PASMC complex III, mitochondria and cells, mediating the hypoxic increase in $[Ca^{2+}]_i$ in PASMCs and hypoxic vasoconstriction in pulmonary arteries.

Materials and Methods

Electron microscopic examination of isolated mitochondria

All the animals were used in accordance with the approved Animal Care and Use Protocol of Albany Medical College. Resistance (third and smaller intralobar) PASM tissues and cells were prepared from Swiss Webster mice, as we reported previously [12;13].

Mitochondria were isolated from PASM tissues by differential centrifugation [14]. All the steps below were performed at 4 °C. Isolated PAs were exposed to papain (0. 5 mg/ml) for 25 min, and placed in an all-glass dounce homogenizer that contained 1 ml isolation buffer consisted of (mM): 215 mannitol, 75 sucrose, 20 4-(2-hydroxyethyl)-1-piperazineethanesulfonic acid (HEPES), 1 ethylene glycol tetraacetic acid (EGTA) and 0.1% bovine serum albumin (BSA, pH 7.2), and homogenized. The homogenate were spun twice at 1,300 × g in an Eppendorf microcentrifuge for 3 min. The resulting supernatant was topped top off with isolation buffer and then spun at 13,000 × g for 10 min. The pellet was re-suspended in 500 μl isolation buffer, and placed inside the nitrogen cell disruption bomb (Parr Instrument) under a pressure of up to 1200 psi for 10 min. The samples were brought up to 2 ml isolation buffer, and centrifuged at 13,000 × g for 10 min. The pellet was re-suspended in isolation buffer and centrifuged at 10,000 × g for 10 min. The collected pellet was re-suspended in isolation buffer to yield the mitochondrial suspension (10 mg protein/ml).

Isolated mitochondria were fixed with 4% paraformaldehyde and 0.25% glutaraldehyde in Sorenson's buffer and infiltrated with LR-White resin using standard procedures. Sections of 15-nm thickness were cut on a Leitz ultramicrotome and collected on nickel grids, and counterstained with uranyl acetate and lead citrate. The grids were examined and photographed on a Hitachi H7100 transmission electron microscope.

Measurement of cytochrome c release in isolated mitochondria

Fifty μL of isolated mitochondrial suspension (10 μg protein) was added in microplate wells that contained 75 μl cytochrome c conjugate (monoclonal antibody against cytochrome c conjugated to horseradish peroxidase). After incubation for 2 h at ~22 °C, 100-μl H_2O_2 (100 μM) and tetrabenazine (1 mM) mixture was added and incubated for 30 min at ~22 °C. The reaction was stopped by adding 100 μl stop solution with 2 N hydrochloric acid. A change in the difference in the absorbance at 450 and 570 nm (A_{450}-A_{570}), measured at 37 °C using a FlexStation-III spectrophotometer (Molecular Devices), was taken as the amount of cytochrome c release [14].

Detection of ROS production

Isolated mitochondrial samples (50 μg protein) were added in microplate wells containing respiration buffer that included 5 mM pyruvate, 2.5 mM malate, 10 μM dichlorodihydrofluorescein diacetate (H_2DCF/DA, Molecular Probes) and 5 μM horseradish peroxidase (HRP). After incubation for 10 min, fluorescence was measured at 37 °C using the FlexStation-III spectrophotometer with an excitation wavelength of 485 nm and emission wavelength of 532 nm. ROS production was determined by subtracting the fluorescence intensity measured in control wells that contained assay buffer without mitochondria [14].

Mitochondrial inter-membrane space ROS generation in isolated PASMCs was assessed using the newly-developed, specific ROS biosensor pHyPer-dMito (exclusively targeted to mitochondrial inner membrane) [15]. Freshly isolated PASMCs were cultured at 37 °C in modified Dulbecco's minimal essential medium (DMEM) containing 10% fetal bovine serum and 1% penicillin/streptomycin. After culture for 48 h at which cells became ~80% confluent, cells were transfected with pHyPer-dMito construct. Following transfection for 72 h, an equal number of cells were added to microplate wells with normal physiological saline solution (PSS). HyPer was alternatively excited at 420 and 500 nm. Emitted fluorescence at 510 nm was measured at 37 °C using the FlexStation-III spectrophotometer.

Measurement of ROS formation in isolated complex III was similar to that in isolated mitochondria, except that 40 μM reduced decylubiquinone, 2 mM potassium cyanide and 50 μM cytochrome *c* were used as substrates instead of pyruvate and malate. Isolated complex III was obtained from isolated PASMC mitochondria using immunocapture kits (Mitoscience) according to the manufacturer's instructions. Isolated mitochondria were incubated in phosphate-buffered saline solution (PBSS) buffer with 20 mM lauryl maltoside and protease inhibitor mixture on ice for 30 min, and centrifuged 72,000 g at 4°C for 10 min. The resulted supernatant was incubated at ~22 °C for 3 h with 10 μl beads that were attached with specific complex III antibodies. Beads were collected by gentle centrifugation at 500 g for 30 seconds and washed using PBSS for 5 min for 3 times. Complex III samples were eluted by adding 50 μl of 1% sodium dodecyl sulfate (SDS). Collected complex III samples were added in respiration buffer containing H_2DCF/DA and HRP. After incubation for 10 min, fluorescence was measured at 37 °C using the FlexStation-III spectrophotometer.

Measurement of mitochondrial ATP production

ATP production was measured using ATP Determination Kit (Molecular Probes) according to the manufacturer's instructions. Isolated mitochondrial samples (10 μg) were added in 500 μL ATP detection buffer. After incubation for 15 min, emitted luminescence at 560 nm was measured at 37 °C using the FlexStation-III spectrophotometer. The background luminescence was read before the addition of samples. The amount of ATP in samples was calculated from the standard curve.

Determination of mitochondrial respiration activity

Mitochondrial respiration activity was determined using a miniature Clark electrode (Hansatech Instruments) in a sealed, thermostated (37 °C) and continuously stirred chamber [14]. Isolated mitochondria (50 μg protein) were added to the chamber with 500 μL respiration buffer contained mM: 215 mannitol, 75 sucrose, 2 $MgCl_2$, 2.5 inorganic phosphates, 20 HEPES and 0.1% fatty acid-free BSA (pH 7.2). State I respiration was determined before addition of any substrate, state II respiration after addition of 5 mM pyruvate and 2.5 mM malate, state III respiration after addition of 1 mM adenosine diphosphate, state IV respiration after addition of 1μg/ml oligomycin, and state V respiration after addition of 1 μM carbonyl cyanide-p-trifluoromethoxyphenylhydrazone. Respiration activity was determined by respiration control ratio between state III and state IV.

Measurement of complex III activity

Isolated complex III samples (5 μg protein) were added in 96 microplate wells that contained 100 μl assay buffer (37 °C) with 40 μM reduced decylubiquinone and 2 mM potassium cyanide. The assay was initiated by adding 50 μM cytochrome *c*. The reduction of cytochrome *c*, taken as the activity of complex III, was measured at 550 nm using the FlexStation-III spectrophotometer.

Western blot analysis

Western blot analysis was performed as described in previous reports [12;13]. Samples (10 μg protein) were loaded onto 12% SDS gels and then transferred nitrocellulose membrane. The membrane was incubated with primary antibodies (Invitrogen) for the complex III subunit Core 1 protein, complex IV subunit COX IV protein or Rieske iron-sulfur protein at a dilution of 1:2000 followed by appropriate secondary antibodies (Invitrogen) at a dilution of 1:4000. The targeted proteins were probed with an enhanced chemiluminescence detection kit (Santa Cruz) and quantified using Multi Gauge software (Fujifilm).

Rieske iron-sulfur protein silencing and overexpression

Specific siRNAs for Rieske iron-sulfur protein with the sequence of “AAG GUG CCU GAC UUC UCU GAA” were obtained from Dharmacon. One μg siRNAs and 6 μl Lipofectamine 2000 were mixed in 3 ml Opti-MEM medium (Invitrogen) for 15 min at ~22 °C (which helps siRNAs enter cells), and then applied to primary cultured PASMCs [16]. Cells were cultured in a 5% CO_2 incubator at 37°C for 72 h. As control, cells were treated identically, but either untransfected or transfected with scrambled siRNA with the sequence of “GCU UAC UGC GUA UAG GUC ACA”.

To silence Rieske iron-sulfur protein expression in isolated PAs, siRNAs for Rieske iron-sulfur protein were introduce into tissues using reverse permeabilization, as described earlier [17]. Isolated PAs were transferred to culture dishes and exposed to the following three successive solutions (4 °C) containing (in mM): 1) 10 EGTA, 120 KCl, 5 ATP, 2 $MgCl_2$, 20 TES (pH 6.80 for 20 min; 2) 120 KCl, 5 ATP, 2 $MgCl_2$, and 20 TES and 20 nM siRNAs (pH 6.8) for 3 h; and 3) 120 KCl, 5 ATP, 10 $MgCl_2$, and 20 TES and 20 nM siRNAs (pH

6.8) for 30 min. Subsequently, PAs were bathed in a fourth solution containing (in mM): 140 NaCl, 5 KCl, 10 $MgCl_2$, 5 glucose, and 2 MOPS (pH 7.1, 22°C) in which extracellular Ca^{2+} concentration was gradually increased from 0.01 to 0.1 to 1.8 mM every 15 min. Following this, PAs were placed in DMEM/F-12 medium (supplemented with 1 mM L-glutamine, 50 U/ml penicillin and 50 μg/ml streptomycin) and cultured at 37 °C for 72 h. As control, PAs were treated similarly, but untreated with siRNAs for Rieske iron-sulfur protein or treated with scrambled siRNAs.

In Rieske iron-sulfur protein overexpression studies, primary cultured cells were transfected with pCMV-XL4 vector containing Rieske iron-sulfur gene (Origene), untransfected or transfected with expression vector alone for 72 h.

The efficiency of Rieske iron-sulfur protein silencing and overexpression were determined using Western blot analysis, as described above.

Measurement of $[Ca^{2+}]_i$

As described in our previous reports [12;18], cells were incubated with 10 μM fura-2/AM at 37 °C for 30 min. Fura-2 was excited at 340 and 380 nm with the FlexStation-III spectrophotometer, and emitted fluorescence detected at 510 nm.

Muscle tension measurement

Muscle tension in isolated PA rings was measured as described earlier [12;13]. PA rings with 3 mm in length were placed in 2 ml tissue bath (Radnoti) at 37 °C. All the PAs used were devoid of the endothelium. The absence of the endothelium was confirmed by the lack of 10 μM methacholine-evoked relaxation. Passive tension of 200 mg was applied to each of the PA rings. Viability of PAs was tested with 10 μM phenylephrine. Experiments started after an equilibration period for 90 min. Contraction recordings were made using a highly sensitive force transducer (Harvard Apparatus) with a Powerlab/4SP recording system (AD Instruments).

Hypoxia

To induce hypoxic responses in isolated complex III, mitochondria and cells, the medium used was first aerated with 20% O_2, 5% CO_2 and 75% N_2 mixture (normoxic gas) for 10 min and then with 1% O_2, 5% CO_2 and 96% N_2 mixture (hypoxic gas) for 5 min to induce hypoxic responses, as we reported previously [7-9;12;13;18-20]. As control, samples were treated with normoxic gas alone. To assess HPV, isolated PA rings were equilibrated with the abovementioned normoxic gas for 90 min and then exposed to hypoxic for up to 45 min. Oxygen tension in normoxic and hypoxic bath solutions were determined using an OXEL-1 oxygen electrode connected to an ISO_2 isolated dissolved oxygen meter (World Precision Instruments).

Statistical analysis

Data are expressed as means ± standard error of the mean obtained from at least 3 independent experiments. Student's *t* test or one-way ANOVA with Bonferroni post hoc test was used to determine the significance of differences between comparisons. A $P < 0.05$ was accepted as statistically significant.

Results

Hypoxia causes an increase in ROS generation in isolated mitochondria from PASMCs

Mitochondria in PASMCs are considered to be implicated in hypoxic sensing to enhance ROS generation, leading to HPV [1-6]. To provide direct experimental evidence for this view, we sought to determine whether hypoxia could directly affect ROS production in isolated mitochondria from PASMCs. Electron microscopic studies showed that isolated mitochondria had the well preserved structures (Fig. 1A). Application of Triton X-100 (1 mM) caused a massive cytochrome c release (Fig. 1B). These data indicate that the isolated mitochondria are intact and viable.

Excitingly, for the first time, we have found that acute hypoxic exposure for 5 min significantly enhanced ROS production, determined using the classic ROS detection probe dichlorodihydrofluorescein/diacetate (H_2DCF/DA), in isolated mitochondria (Fig. 1C). However, hypoxia did not affect mitochondrial ATP production (Fig. 1D). Mitochondrial oxygen consumption was not affected, either (Fig. 1E). In these experiments, the mean O_2 tension in normoxic and hypoxic solutions in the recording tube were 160.1 ± 9.0 and 12.8 ± 3.4 mmHg, respectively.

Using pHyPer-dMito, an expression vector that encodes newly-developed, specific ROS detection biosensor HyPer and is exclusively targeted in the mitochondrial inner membrane [15], we further revealed that hypoxia causes a large increase in HyPer-derived fluorescence ($[ROS]_i$) in PASMCs (Fig. 1F). These findings are consistent with our previous reports using the traditional ROS detection approaches [7-9;18]. As control experiments, we also assessed the effect of exogenous H_2O_2 on HyPer-derived fluorescence in PASMCs. The results indicated that H_2O_2 could result in a concentration-dependent increase in HyPer signals (Fig. 1G).

Hypoxia enhances ROS formation in isolated complex III from PASMCs

Pharmacological studies imply that the hypoxic ROS production in PASMCs predominantly occurs at the mitochondrial ETC complex III [1]. Consistent with previous data, here we unveiled that acute hypoxia largely enhanced ROS generation in isolated complex III from PASMCs (Fig. 2A). The isolated complex III had a high purity, as Western blot analysis showed the presence of the complex III subunit Core 1 protein, but not the complex IV subunit COX IV protein in isolated complex III preparations (Fig. 2B).

Interestingly, the activity of isolated complex III was remarkably enhanced as well (Fig. 2C). These data provide the novel evidence that hypoxia may enhance the functional activity of the complex III and then its ROS formation, leading to an increase in $[ROS]_i$ in PASMCs.

Rieske iron-sulfur protein silencing blocks the hypoxic ROS generation in isolated PASM complex III, mitochondria and cells

Rieske iron-sulfur protein is an important functional component in the complex III [11]. Thus, we wondered whether this molecule is required for the hypoxic ROS generation in complex III of PASMCs. Our data indicate that transfection with specific siRNAs for Rieske iron-sulfur protein suppressed its expression in isolated PASMCs by 90% (Fig. 3A). However, transfection with scrambled siRNAs had no effect.

Transfection of siRNAs for Rieske iron-sulfur protein could decrease the basal activity of isolated complex III from PASMCs (Fig. 3B). Importantly, siRNAs for Rieske iron-sulfur protein, but not scrambled siRNAs, completely prevented acute hypoxia from enhancing the activity of isolated complex III. Rieske iron-sulfur protein silencing also moderately

inhibited the basal ROS generation and fully abolished the hypoxic ROS formation in isolated complex III (Fig. 3C). Consistent with its direct effect, hypoxia did not alter Rieske iron-sulfur protein expression in PASMCs (Fig. 3D).

Rieske iron-sulfur protein overexpression augments the hypoxic ROS generation in isolated PASM complex III, mitochondria and cells

Transfection with Rieske iron-sulfur gene, but not expression vector alone, significantly augmented its protein overexpression in isolated PASMCs (Fig. 4A).

In contrast to its silencing, Rieske iron-sulfur protein overexpression could increase the basal activity as well as hypoxic increase in the activity of isolated complex III (Fig. 4B). Moreover, Rieske iron-sulfur protein overexpression also enhanced the hypoxic ROS generation in isolated complex III (Fig. 4C).

Rieske iron-sulfur protein silencing prevents, whereas Rieske iron-sulfur protein overexpression enhances the hypoxic ROS generation in isolated PASM mitochondria and cells

Compatible with the effect in isolated complex III, Rieske iron-sulfur protein silencing reduced the basal ROS generation and blocked the hypoxic ROS generation in isolated mitochondria (Fig. 5A). The hypoxic increase in mitochondrial ROS generation, determined using HyPer, was inhibited as well in PASMCs (Fig. 5B).

As expected, Rieske iron-sulfur protein overexpression was able to enhance the basal ROS generation as well as hypoxic ROS generation in isolated PASM mitochondria (Fig. 5C) and cells (Fig. 5D).

Rieske iron-sulfur protein silencing inhibits the hypoxic increase in $[Ca^{2+}]_i$ in PASMCs and HPV

Introduction of siRNAs for Rieske iron-sulfur protein into isolated PAs using reverse permeabilization [17] largely suppressed its protein expression (Fig. 6A). In line with this result, introduction of siRNAs for Rieske iron-sulfur protein markedly reduced HPV (Fig. 6B). On the other hand, scrambled siRNAs had no effect. In these studies, the mean O_2 tension in normoxic and hypoxic solutions in the tissue bath were 155.5 ± 11.5 and 14.2 ± 4.1 mmHg, respectively.

Similar to our previous findings [7-9;12;13;18-20], hypoxia caused a large increase in $[Ca^{2+}]_i$ in PASMCs. The hypoxic increase in $[Ca^{2+}]_i$ was mostly blocked by Rieske iron-sulfur protein silencing. The mean increase in $[Ca^{2+}]_i$ was decreased from 671.0 ± 35.5 nM in control (untransfected) cells to 173.3 ± 9.7 nM in cells transfected with siRNAs for Rieske iron-sulfur protein (Fig. 6C). In control experiments, transfection with scrambled siRNAs did not produce an effect.

Discussion

Based on previous pharmacological data in cells and tissues, we and others have proposed that mitochondria are implicated in hypoxic sensing to affect their ROS generation, mediating the hypoxic increase in $[Ca^{2+}]_i$ in PASMCs and associated HPV [1-6]. As this long-standing conjecture lacks the support of direct experimental evidence, we have contemplated whether hypoxia may cause an increase in ROS production in isolated mitochondria from PASMCs. The findings presented in this study, for the first time, reveal that mitochondria can directly respond to hypoxia to produce ROS in PASMCs. Reports from our laboratory and many others have shown that hypoxia causes an increase in $[ROS]_i$

in isolated PASMCs, PAs and lungs, while a few research groups have reported that hypoxia decreases, rather than increases $[ROS]_i$ [1-6]. These inconsistent results have been thought to be attributed to the potentially dissimilar hypoxic responses between single cells and multiple-cell tissues and between freshly isolated and passaged cells [21;22]. The freshly isolated mitochondria are devoid of these possible problems and thus can be considered as reliable preparations for studies of direct hypoxic sensing. It is also worthy to point out that by making simultaneous measurement of H_2DCF-derived fluorescence signal and staining of mitochondria, we have found that the hypoxic ROS generation in mitochondrial areas is earlier and larger than that in non-mitochondrial and whole cell areas [8]. These data, together with the hypoxic ROS generation in isolated mitochondria (this study) and intact mitochondria of PASMCs [23], fully support the role of mitochondria in hypoxic sensing in PASMCs.

The site for the hypoxic generation of mitochondrial ROS in PASMCs is uncertain. Using mitochondrial ETC complex I, III and IV inhibitors, earlier investigations by Archer *et al* suggest that hypoxia could decrease ROS production at complex I and/or III, leading to HPV [24;25]. However, a number of later studies by several different laboratories using complex inhibitors imply that complex III is the major site of the hypoxic ROS production to cause an increase in $[Ca^{2+}]_i$ in PASMCs and HPV [8;26-29]. Moreover, it has also reported that complex I, II, III and IV are all likely to be involved in HPV [30-33]. Noticeably, our work further indicates that the ETC molecules prior to the complex III ubisemiquinone site may act as a functional unit to mediate the hypoxic ROS generation at complex III in PASMCs, as simultaneous treatment with complex I and II inhibitors, I and III pre-ubisemiquinone site inhibitors, as well as II and III pre-ubisemiquinone site inhibitors neither have additive effects on the hypoxic increase in $[ROS]_i$ nor $[Ca^{2+}]_i$ [8]. Here, we have found that hypoxia significantly enhances ROS formation in isolated complex III. This novel result demonstrates that the mitochondrial complex III has an inherent hypoxic sensing capability. In addition, we have revealed that hypoxia does not alter mitochondrial ATP production and respiration. These data, together with the hypoxic ROS generation in isolated complex III, indicate that mitochondrial hypoxic sensing does not necessarily depend on the reduced availability of oxygen at cytochrome c and electron flux through the ETC, at least in PASMCs. In essence, we have provided the first evidence-based proof for the original hypothesis by Schumacker and his associates that the complex III is not only the source of ROS signals, but also the oxygen sensor per se [6]. Interestingly, our data further disclose that the activity of isolated complex III, similar to ROS formation, is also significantly enhanced by hypoxia. Thus, the complex III ROS formation is likely to be dependent on its activity, supporting previous reports that pharmacological inhibitors that block the complex III activity can prevent the hypoxic ROS generation in PASMCs, PAs and lungs [1-3;5].

Rieske iron-sulfur protein is a component of complex III and critical for its functional activity [11]; accordingly, we investigated its potential role in the hypoxic ROS generation in PASMCs. Using siRNA technology, we have found that Rieske iron-sulfur protein silencing completely blocks the hypoxic increase in isolated complex III activity and ROS formation. Likewise, the hypoxic ROS production in isolated PASM mitochondria and cells are fully abolished by Rieske iron-sulfur protein silencing. In line with its silencing, Rieske iron-sulfur protein overexpression significantly augments the hypoxic ROS formation in isolated complex III, mitochondria and PASMCs. Moreover, Rieske iron-sulfur protein silencing reduces, while Rieske iron-sulfur protein overexpression increases, the basal activity of isolated complex III and basal ROS production in isolated complex III and mitochondria. These results, together with previous publications that Rieske iron-sulfur protein silencing blocks hypoxic cellular responses in mammalian cell lines and yeast [34-39], further support the view that complex III is implicated in hypoxic sensing, and suggest that Rieske iron-sulfur protein plays an important role in the basal and hypoxic ROS

production in PASMCs. Complex III is known to carry out the ubiquinone (Q) cycle to transport electrons from the complex I or II to complex IV. Ubiquinone at complex III's Qo site accepts a pair of reducing equivalents, becoming ubihydroquinone. Rieske iron-sulfur protein can seize a single electron from ubihydroquinone through its extrinsic domain and pass it to the cytochrome c1 due to the movement of the extrinsic domain. Meanwhile, ubihydroquinone becomes ubisemiquinone, which transfers its electron to the cytochrome b (from b_{566} to b_{562}) and then to another ubisemiquinone at the Qi site to regenerate ubiquinone. During this process, a small fraction of electrons may escape from ubisemiquinone to oxygen to form a superoxide anion at the Qo and also possibly at the Qi site [6;11;40;41]. As such, we speculate that hypoxia may perhaps affect the function of Rieske iron-sulfur protein in transferring electron from ubihydroquinone to cytochrome c1, leading to an increase in the electron transfer rates and ROS formation in complex III. Apparently, it would be very interesting to test this exciting hypothesis in future studies. A recent, elegant study has shown that ubiquinol-cytochrome c reductase binding (UQCRB) protein, an element of complex III, is involved in the hypoxic ROS generation to mediate breast cancer angiogenesis [42]. This raises a possibility that hypoxia may enhance the activity of UQCRB protein, thereby causing ROS generation in PASMCs.

As ROS mediate the hypoxic increase in $[Ca^{2+}]_i$ in PASMCs and HPV [1-6], Rieske iron-sulfur protein is possibly imperative for these hypoxic responses as well. Indeed, Rieske iron-sulfur protein silencing significantly inhibits the hypoxic increase in $[Ca^{2+}]_i$ in PASMCs. Moreover, we have for the first time shown that Rieske iron-sulfur protein siRNAs can be introduced into isolated PAs by a reverse permeabilization approach, causing a large reduction in HPV.

In conclusion, hypoxia can directly cause ROS generation in isolated complex III and mitochondria from PASMCs. The hypoxic ROS generation is blocked by Rieske iron-sulfur protein silencing, whereas augmented by Rieske iron-sulfur protein overexpression. Furthermore, Rieske iron-sulfur protein silencing inhibits the hypoxic increase in $[Ca^{2+}]_i$ in PASMCs and HPV. These findings, for the first time, provide clear evidence that Rieske iron-sulfur protein is likely to be an essential, primary molecule in the hypoxic ROS generation, leading to an increase in $[Ca^{2+}]_i$ in PASMCs, and ultimately pulmonary vasoconstriction.

Acknowledgments

This work was supported by AHA Established Investigator Award 0340160N and NIH R01HL64043, HL064043-S1 and HL075190 (Y.-X. W.), as well as AHA Scientist Development Grant 0630236N (Y.-M. Z.).

List of Abbreviations

BSA	bovine serum albumin
ETC	Electron transport chain
H_2DCF/DA	5,6-chloromethyl-2,7-dichlorodihydrofluorescein diacetate
DMEM	modified Dulbecco's minimal essential medium
EGTA	ethylene glycol tetraacetic acid
GAPDH	glyceraldehyde 3-phosphate dehydrogenase
HEPES	4-(2-hydroxyethyl)-1-piperazineethanesulfonic acid
HPV	hypoxic pulmonary vasoconstriction

HRP	horseradish peroxidase
NOX	NADPH oxidase
PA	pulmonary artery
PBSS	phosphate-buffered saline solution
PSS	physiological saline solution
SDS	sodium dodecyl sulfate
SMCs	smooth muscle cells
ROS	reactive oxygen species
TBST	Tris-buffered saline with Tween-20

References

1. Wang YX, Zheng YM. ROS-dependent signaling mechanisms for hypoxic Ca^{2+} responses in pulmonary artery myocytes. Antioxid Redox Signal 2010;12:611–623. [PubMed: 19764882]
2. Ward JP, McMurtry IF. Mechanisms of hypoxic pulmonary vasoconstriction and their roles in pulmonary hypertension: new findings for an old problem. Curr Opin Pharmacol 2009;9:287–296. [PubMed: 19297247]
3. Waypa GB, Schumacker PT. Oxygen sensing in hypoxic pulmonary vasoconstriction: using new tools to answer an age-old question. Exp Physiol 2008;93:133–138. [PubMed: 17993507]
4. Sommer N, Dietrich A, Schermuly RT, Ghofrani HA, Gudermann T, Schulz R, Seeger W, Grimminger F, Weissmann N. Regulation of hypoxic pulmonary vasoconstriction: basic mechanisms. Eur Respir J 2008;32:1639–1651. [PubMed: 19043010]
5. Archer SL, Gomberg-Maitland M, Maitland ML, Rich S, Garcia JG, Weir EK. Mitochondrial metabolism, redox signaling, and fusion: a mitochondria-ROS-HIF-1alpha-K_V1.5 O_2-sensing pathway at the intersection of pulmonary hypertension and cancer. Am J Physiol Heart Circ Physiol 2008;294:H570–H578. [PubMed: 18083891]
6. Guzy RD, Schumacker PT. Oxygen sensing by mitochondria at complex III: the paradox of increased reactive oxygen species during hypoxia. Exp Physiol 2006;91:807–819. [PubMed: 16857720]
7. Rathore R, Zheng YM, Li XQ, Wang QS, Liu QH, Ginnan R, Singer HA, Ho YS, Wang YX. Mitochondrial ROS-PKCε signaling axis is uniquely involved in hypoxic increase in $[Ca^{2+}]_i$ in pulmonary artery smooth muscle cells. Biochem Biophys Res Commun 2006;351:784–790. [PubMed: 17087917]
8. Wang QS, Zheng YM, Dong L, Ho YS, Guo Z, Wang YX. Role of mitochondrial reactive oxygen species in hypoxia-dependent increase in intracellular calcium in pulmonary artery myocytes. Free Radic Biol Med 2007;42:642–653. [PubMed: 17291988]
9. Rathore R, Zheng YM, Niu CF, Liu QH, Korde A, Ho YS, Wang YX. Hypoxia activates NADPH oxidase to increase $[ROS]_i$ and $[Ca^{2+}]_i$ through the mitochondrial ROS-PKCε signaling axis in pulmonary artery smooth muscle cells. Free Radic Biol Med 2008;45:1223–1231. [PubMed: 18638544]
10. Murphy MP. How mitochondria produce reactive oxygen species. Biochem J 2009;417:1–13. [PubMed: 19061483]
11. Berry EA, Guergova-Kuras M, Huang LS, Crofts AR. Structure and function of cytochrome bc complexes. Annu Rev Biochem 2000;69:1005–1075. [PubMed: 10966481]
12. Zheng YM, Mei QB, Wang QS, Abdullaev I, Lai FA, Xin HB, Kotlikoff MI, Wang YX. Role of FKBP12.6 in hypoxia- and norepinephrine-induced Ca^{2+} release and contraction in pulmonary artery myocytes. Cell Calcium 2004;35:345–355. [PubMed: 15036951]
13. Zheng YM, Wang QS, Rathore R, Zhang WH, Mazurkiewicz JE, Sorrentino V, Singer HA, Kotlikoff MI, Wang YX. Type-3 ryanodine receptors mediate hypoxia-, but not neurotransmitter-

induced calcium release and contraction in pulmonary artery smooth muscle cells. J Gen Physiol 2005;125:427–440. [PubMed: 15795312]

14. Korde AS, Pettigrew LC, Craddock SD, Maragos WF. The mitochondrial uncoupler 2,4-dinitrophenol attenuates tissue damage and improves mitochondrial homeostasis following transient focal cerebral ischemia. J Neurochem 2005;94:1676–1684. [PubMed: 16045446]
15. Belousov VV, Fradkov AF, Lukyanov KA, Staroverov DB, Shakhbazov KS, Terskikh AV, Lukyanov S. Genetically encoded fluorescent indicator for intracellular hydrogen peroxide. Nat Methods 2006;3:281–286. [PubMed: 16554833]
16. Xiao JH, Zheng YM, Liao B, Wang YX. Functional role of canonical transient receptor potential 1 and canonical transient receptor potential 3 in normal and asthmatic airway smooth muscle cells. Am J Respir Cell Mol Biol 2010;43:17–25. [PubMed: 19648473]
17. Corteling RL, Brett SE, Yin H, Zheng XL, Walsh MP, Welsh DG. The functional consequence of RhoA knockdown by RNA interference in rat cerebral arteries. Am J Physiol Heart Circ Physiol 2007;293:H440–H447. [PubMed: 17369454]
18. Liao B, Zheng YM, Yadav VR, Korde AS, Wang YX. Hypoxia induces intracellular Ca^{2+} release by causing ROS-mediated dissociation of FKBP12.6 with ryanodine receptor 2 in pulmonary artery myocytes. Antioxid Redox Signal 2011;14:37–47. [PubMed: 20518593]
19. Zheng YM, Wang QS, Liu QH, Rathore R, Yadav V, Wang YX. Heterogeneous gene expression and functional activity of ryanodine receptors in resistance and conduit pulmonary as well as mesenteric artery smooth muscle cells. J Vasc Res 2008;45:469–479. [PubMed: 18434746]
20. Li XQ, Zheng YM, Rathore R, Ma J, Takeshima H, Wang YX. Genetic evidence for functional role of ryanodine receptor 1 in pulmonary artery smooth muscle cells. Pflugers Arch 2009;457:771–783. [PubMed: 18663468]
21. Sham JS. Hypoxic pulmonary vasoconstriction: ups and downs of reactive oxygen species. Circ Res 2002;91:649–651. [PubMed: 12386138]
22. Moudgil R, Michelakis ED, Archer SL. Hypoxic pulmonary vasoconstriction. J Appl Physiol 2005;98:390–403. [PubMed: 15591309]
23. Waypa GB, Marks JD, Guzy R, Mungai PT, Schriewer J, Dokic D, Schumacker PT. Hypoxia triggers subcellular compartmental redox signaling in vascular smooth muscle cells. Circ Res 2010;106:526–535. [PubMed: 20019331]
24. Archer SL, Huang J, Henry T, Peterson D, Weir EK. A redox-based O2 sensor in rat pulmonary vasculature. Circ Res 1993;73:1100–1112. [PubMed: 8222081]
25. Michelakis ED, Hampl V, Nsair A, Wu X, Harry G, Haromy A, Gurtu R, Archer SL. Diversity in mitochondrial function explains differences in vascular oxygen sensing. Circ Res 2002;90:1307–1315. [PubMed: 12089069]
26. Waypa GB, Chandel NS, Schumacker PT. Model for hypoxic pulmonary vasoconstriction involving mitochondrial oxygen sensing. Circ Res 2001;88:1259–1266. [PubMed: 11420302]
27. Waypa GB, Marks JD, Mack MM, Boriboun C, Mungai PT, Schumacker PT. Mitochondrial reactive oxygen species trigger calcium increases during hypoxia in pulmonary arterial myocytes. Circ Res 2002;91:719–726. [PubMed: 12386149]
28. Waypa GB, Guzy R, Mungai PT, Mack MM, Marks JD, Roe MW, Schumacker PT. Increases in mitochondrial reactive oxygen species trigger hypoxia-induced calcium responses in pulmonary artery smooth muscle cells. Circ Res 2006;99:970–978. [PubMed: 17008601]
29. Leach RM, Hill HS, Snetkov VA, Robertson TP, Ward JP. Divergent roles of glycolysis and the mitochondrial electron transport chain in hypoxic pulmonary vasoconstriction of the rat: identity of the hypoxic sensor. J Physiol 2001;536:211–224. [PubMed: 11579170]
30. Weissmann N, Ebert N, Ahrens M, Ghofrani HA, Schermuly RT, Hänze J, Fink L, Rose F, Conzen J, Seeger W, Grimminger F. Effects of mitochondrial inhibitors and uncouplers on hypoxic vasoconstriction in rabbit lungs. Am J Respir Cell Mol Biol 2003;29:721–732. [PubMed: 12791676]
31. Paddenberg R, Ishaq B, Goldenberg A, Faulhammer P, Rose F, Weissmann N, Braun-Dullaeus RC, Kummer W. Essential role of complex II of the respiratory chain in hypoxia-induced ROS generation in the pulmonary vasculature. Am J Physiol Lung Cell Mol Physiol 2003;284:L710–L719. [PubMed: 12676762]

32. Weissmann N, Zeller S, Schäfer RU, Turowski C, Ay M, Quanz K, Ghofrani HA, Schermuly RT, Fink L, Seeger W, Grimminger F. Impact of mitochondria and NADPH oxidases on acute and sustained hypoxic pulmonary vasoconstriction. Am J Respir Cell Mol Biol 2006;34:505–513. [PubMed: 16357364]
33. Sommer N, Pak O, Schörner S, Derfuss T, Krug A, Gnaiger E, Ghofrani HA, Schermuly RT, Huckstorf C, Seeger W, Grimminger F, Weissmann N. Mitochondrial cytochrome redox states and respiration in acute pulmonary oxygen sensing. Eur Respir J 2010;36:1056–1066. [PubMed: 20516051]
34. Guzy RD, Hoyos B, Robin E, Chen H, Liu L, Mansfield KD, Simon MC, Hammerling U, Schumacker PT. Mitochondrial complex III is required for hypoxia-induced ROS production and cellular oxygen sensing. Cell Metab 2005;1:401–408. [PubMed: 16054089]
35. Comellas AP, Dada LA, Lecuona E, Pesce LM, Chandel NS, Quesada N, Budinger GR, Strous GJ, Ciechanover A, Sznajder JI. Hypoxia-mediated degradation of Na,K-ATPase via mitochondrial reactive oxygen species and the ubiquitin-conjugating system. Circ Res 2006;98:1314–1322. [PubMed: 16614303]
36. Bell EL, Chandel NS. Genetics of mitochondrial electron transport chain in regulating oxygen sensing. Methods Enzymol 2007;435:447–461. [PubMed: 17998068]
37. Dada LA, Novoa E, Lecuona E, Sun H, Sznajder JI. Role of the small GTPase RhoA in the hypoxia-induced decrease of plasma membrane Na,K-ATPase in A549 cells. J Cell Sci 2007;120:2214–2222. [PubMed: 17550967]
38. Bell EL, Klimova TA, Eisenbart J, Moraes CT, Murphy MP, Budinger GR, Chandel NS. The Qo site of the mitochondrial complex III is required for the transduction of hypoxic signaling via reactive oxygen species production. J Cell Biol 2007;177:1029–1036. [PubMed: 17562787]
39. Guzy RD, Mack MM, Schumacker PT. Mitochondrial complex III is required for hypoxia-induced ROS production and gene transcription in yeast. Antioxid Redox Signal 2007;9:1317–1328. [PubMed: 17627464]
40. Turrens JF. Mitochondrial formation of reactive oxygen species. J Physiol 2003;552:335–344. [PubMed: 14561818]
41. Chandel NS, Budinger GR. The cellular basis for diverse responses to oxygen. Free Radic Biol Med 2007;42:165–174. [PubMed: 17189822]
42. Jung HJ, Shim JS, Lee J, Song YM, Park KC, Choi SH, Kim ND, Yoon JH, Mungai PT, Schumacker PT, Kwon HJ. Terpestacin inhibits tumor angiogenesis by targeting UQCRB of mitochondrial complex III and suppressing hypoxia-induced reactive oxygen species production and cellular oxygen sensing. J Biol Chem 2010;285:11584–11595. [PubMed: 20145250]

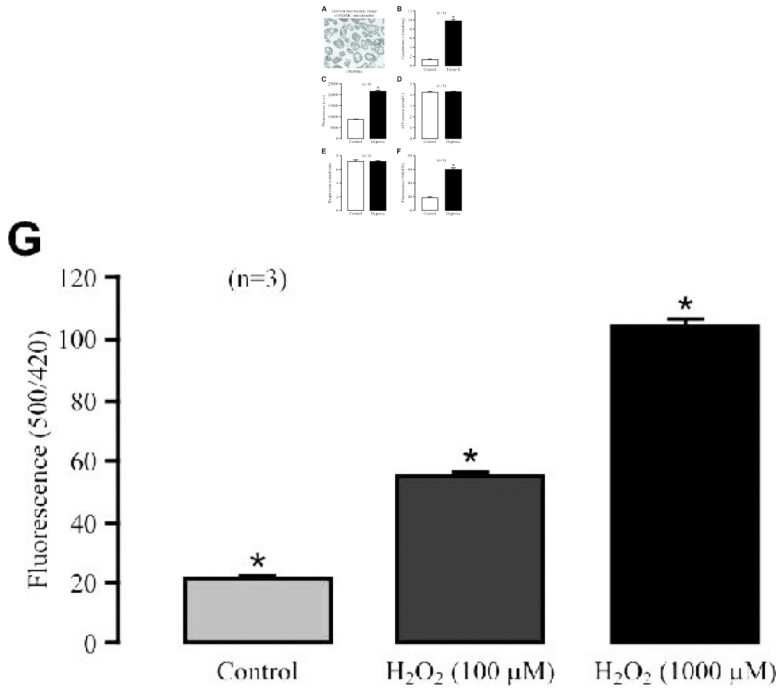

Fig. 1. Hypoxia causes a large increase in ROS production in isolated mitochondria from PASMCs

(A) Representative electron microscopic image of isolated mitochondria. **(B)** Cytochrome c release in isolated mitochondria before and after application of Triton X-100 (1 mM) for 5 min. Numbers in parentheses mean the number of independent experiments performed. **P*<0.05 compared with control (before application of Triton X-100). **(C)** Effect of acute hypoxic exposure for 5 min on ROS production, determined by assessing the fluorescence of the ROS detection dye H_2DCF, in isolated mitochondria. **(D)** Effect of acute hypoxia on ATP production in isolated mitochondria. **(E)** Effect of hypoxia on respiration activity in isolated mitochondria. **(F)** Effect of hypoxia on mitochondrial inter-membrane space ROS production, examined by measuring the fluorescence of the specific ROS biosensor pHyPer, in isolated PASMCs. **(G)** Effect of H_2O_2 on HyPer signals in isolated PASMCs.

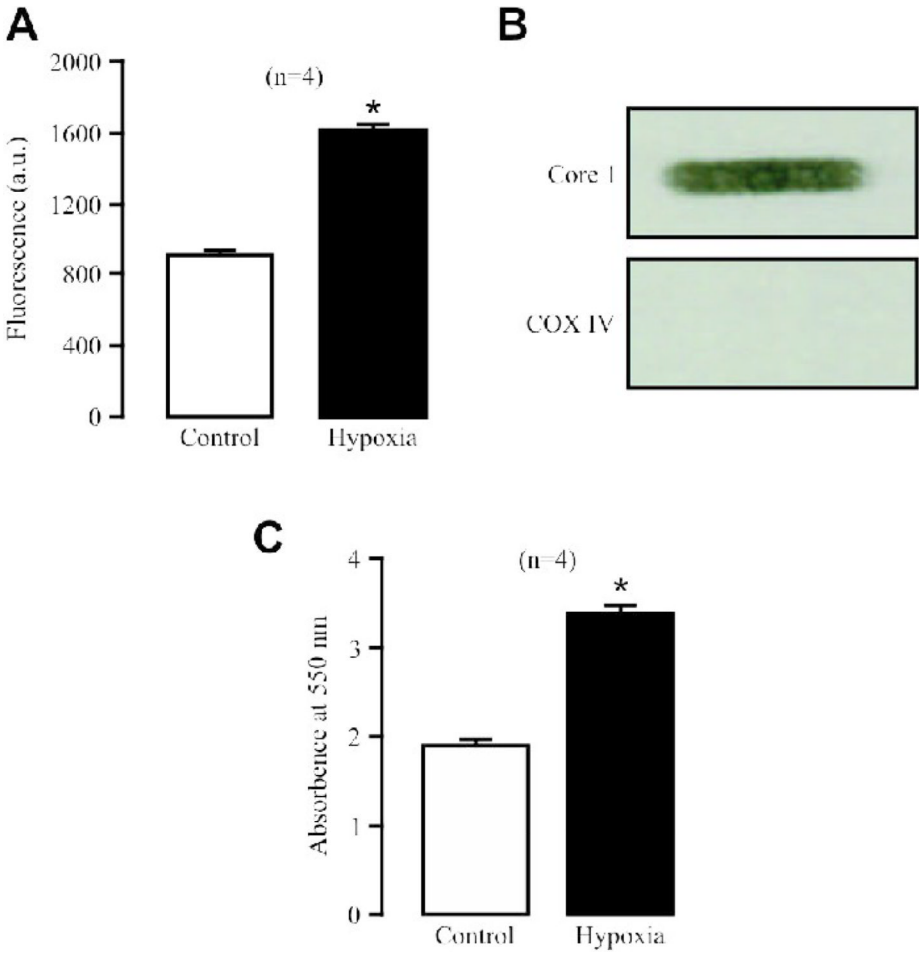

Fig. 2. Hypoxia significantly increases ROS production in isolated complex III from PASMCs

(A) Effect of hypoxia on ROS formation (H_2DCF fluorescence) in isolated complex III. **(B)** Representative Western blots show the presence of the complex III subunit Core 1 protein, but not the complex IV subunit COX IV protein in isolated complex III samples. **(C)** Effect of hypoxia on isolated complex III activity, gauged by assessing the absorbance of cytochrome *c* reduction at 550 nm.

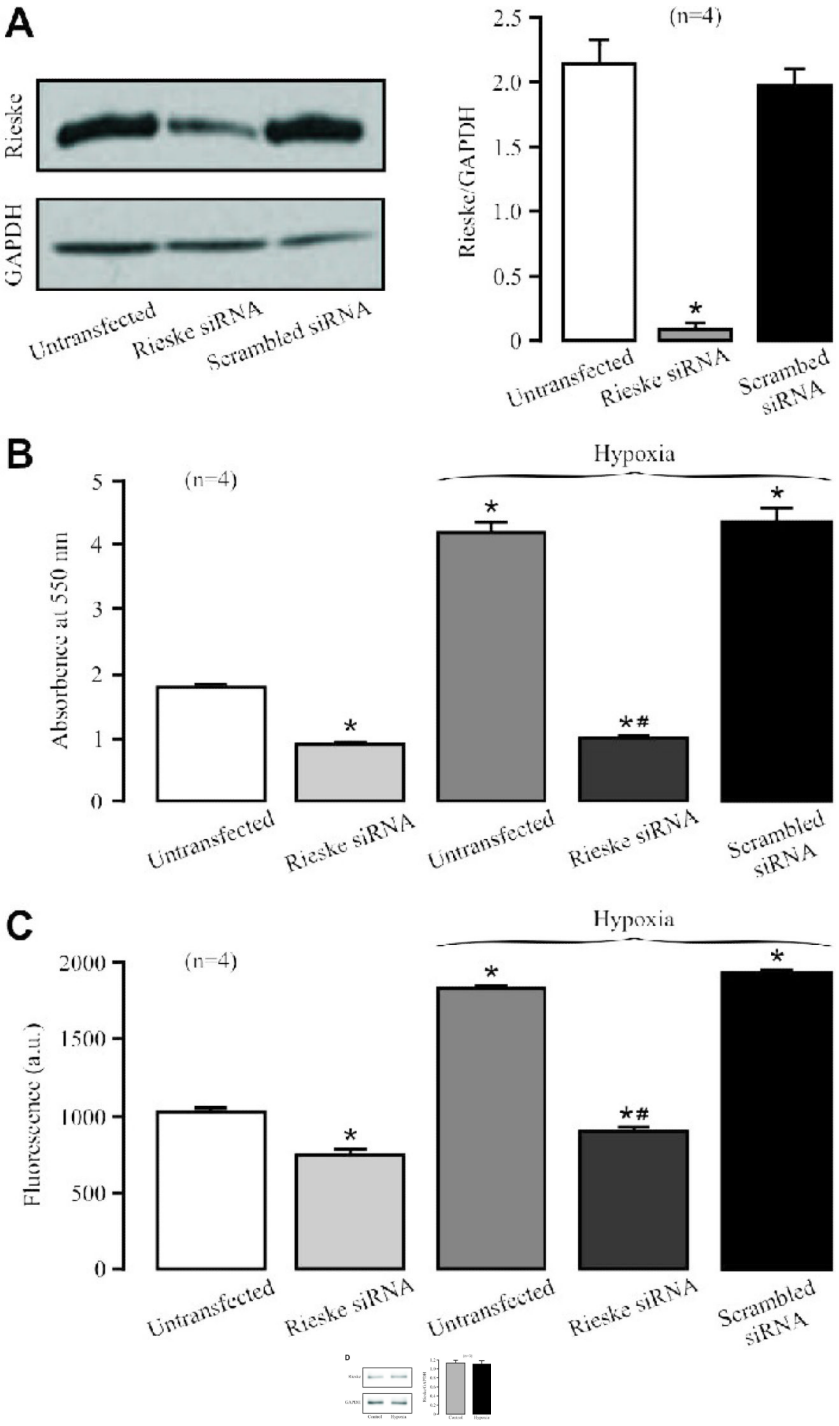

Fig. 3. Rieske iron-sulfur protein silencing blocks the hypoxic ROS production in isolated complex III from PASMCs

(A) Effect of siRNA-mediated Rieske iron-sulfur protein silencing on its protein expression in PASMCs. Representative Western blots illustrate Rieske iron-sulfur protein and glyceraldehyde 3-phosphate dehydrogenase (GAPDH) protein expression in PASMCs untransfected (control) and transfected with Rieske iron-sulfur protein siRNAs or scrambled siRNAs. Bar graph summarizes the effect of Rieske iron-sulfur protein siRNAs on Rieske iron-sulfur protein expression levels. *P<0.05 compared with untransfected cells (control).

(B) Effect of Rieske iron-sulfur protein silencing on the acute hypoxic increase in the activity of isolated complex III. *$P<0.05$ compared with normoxic, untransfected samples; $^{\#}P<0.05$ compared with hypoxic, untransfected samples. **(C)** Effect of Rieske iron-sulfur protein silencing on the hypoxic increase in ROS formation in isolated complex III. **(D)** Effect of acute hypoxia on Rieske iron-sulfur protein expression in PASMCs.

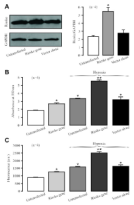

Fig. 4. Rieske iron-sulfur protein overexpression augments the hypoxic ROS generation in complex III from PASMCs

(A) Western blotting images show Rieske iron-sulfur protein and GAPDH protein expression in PASMCs untransfected (control) and transfected with Rieske iron-sulfur gene or expression vector alone. Graph depicts the effect of Rieske iron-sulfur protein overexpression on its protein expression in PASMCs. **(B)** Effect of Rieske iron-sulfur protein overexpression on the hypoxic increase in isolated complex III activity. **(C)** Effect of Rieske iron-sulfur protein overexpression on the hypoxic ROS production in isolated complex III.

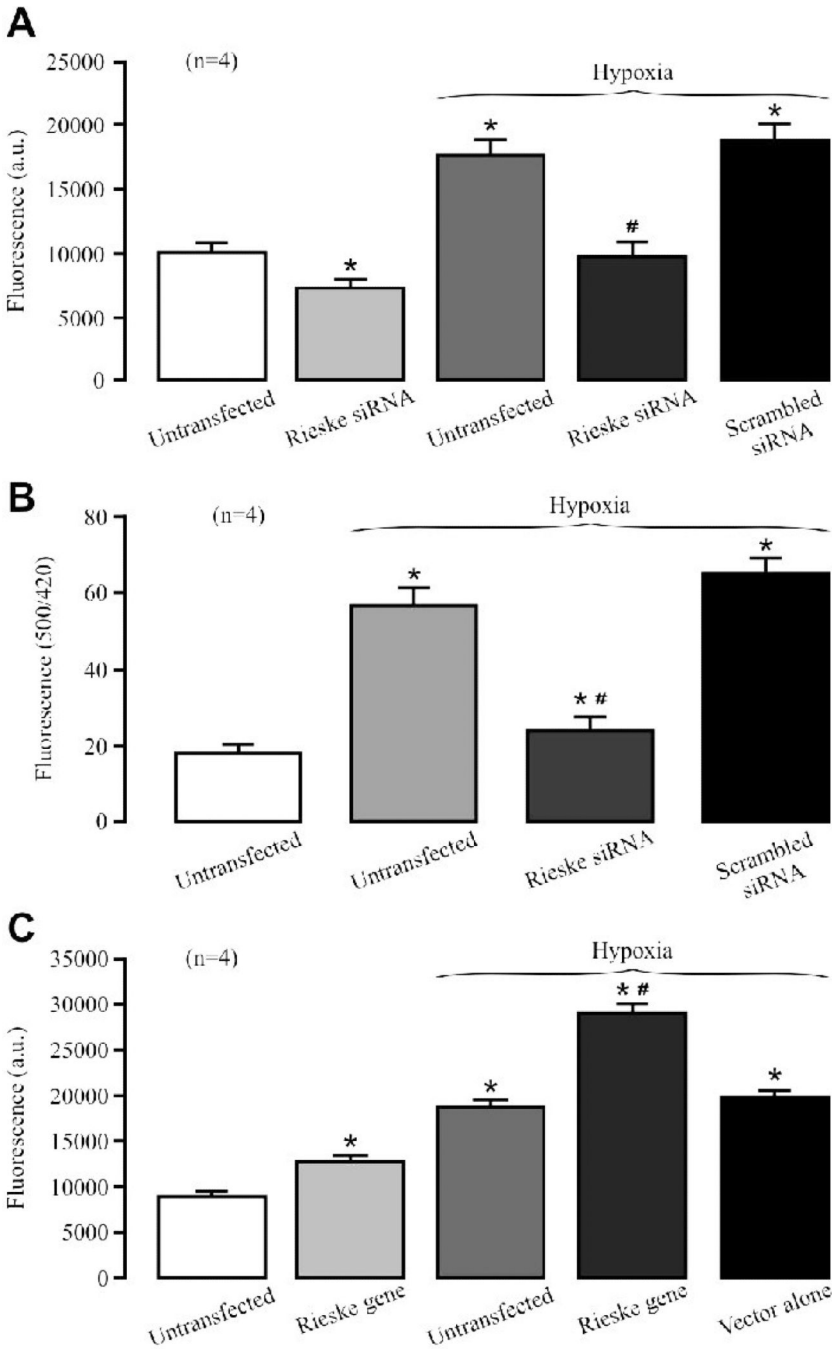

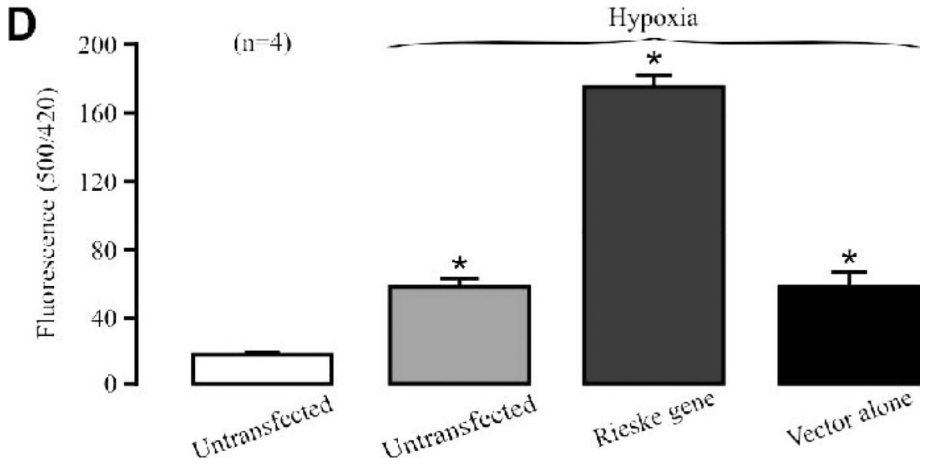

Fig. 5. Rieske iron-sulfur protein silencing prevents, whereas rieske gene overexpression enhances, the hypoxic ROS production in isolated PASM mitochondria and cells

(A) Effect of Rieske iron-sulfur protein silencing on the hypoxic ROS production in isolated mitochondria from PASMCs. **(B)** Effect of Rieske iron-sulfur protein silencing on mitochondrial ROS production in PASMCs. **(C)** Effect of Rieske iron-sulfur protein overexpression on the hypoxic ROS production in isolated mitochondria from PASMCs. **(D)** Effect of Rieske iron-sulfur protein overexpression on mitochondrial ROS production in PASMCs.

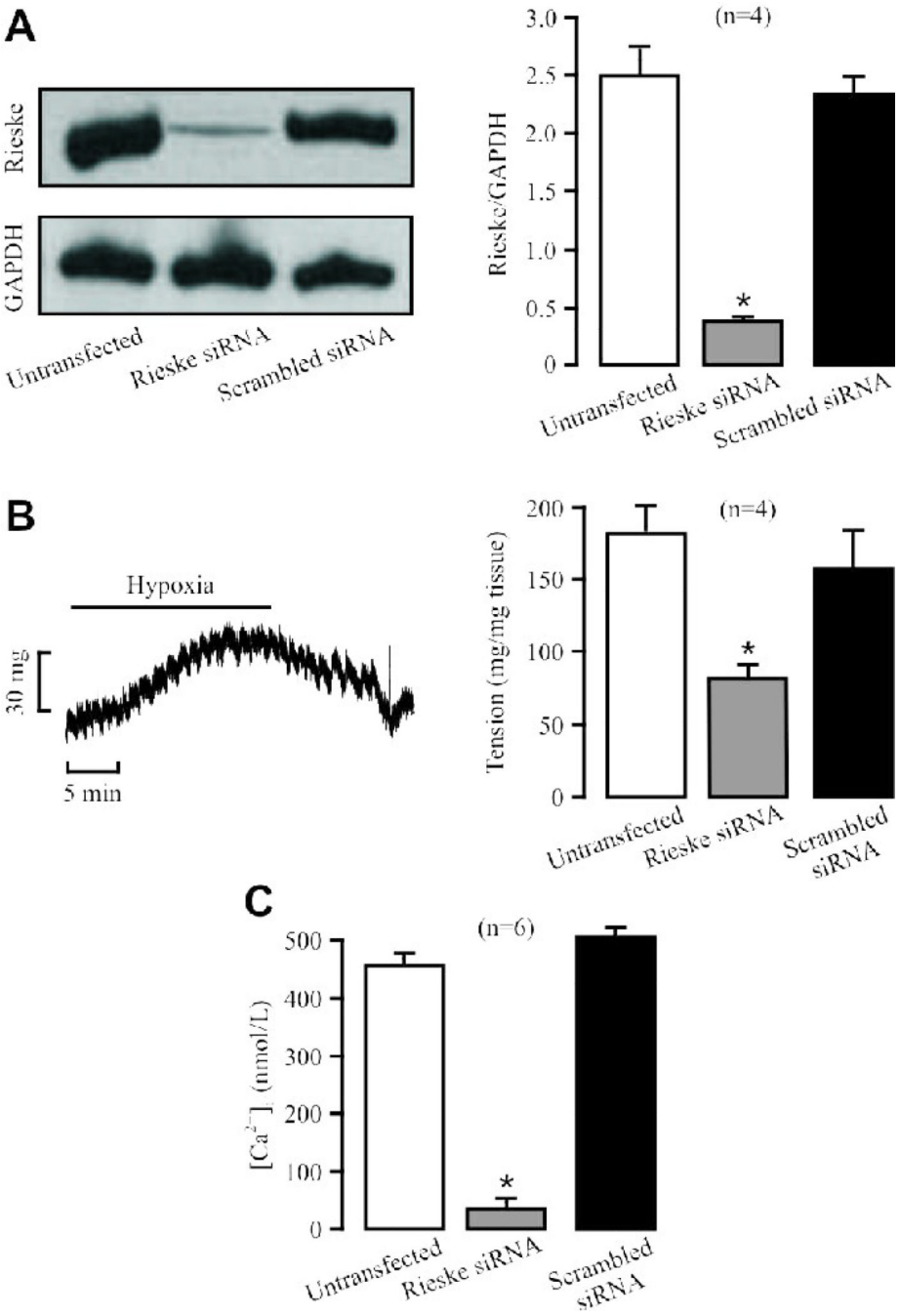

Fig. 6. Rieske iron-sulfur protein silencing inhibits HPV and hypoxic increase in $[Ca^{2+}]_i$ in PASMCs

(A) Representative Western blots show Rieske iron-sulfur protein expression in PAs untransfected (control) and transfected with Rieske iron-sulfur protein siRNAs by reverse permeabilization. Bar graph summarizes the effect of Rieske iron-sulfur protein and scrambled siRNAs on Rieske iron-sulfur protein expression levels. **(B)** A representative recording illustrates hypoxic vasoconstriction in an isolated pulmonary artery. Graph shows the effect of Rieske iron-sulfur protein silencing on HPV. **(C)** Effect of Rieske iron-sulfur protein silencing on the hypoxic increase in $[Ca^{2+}]_i$ in PASMCs. The Number in parenthesis indicates the number of independent experiments performed from 3 separate preparations.